

Evidence for an intramolecular transition metal Arbuzov reaction

Zhao Chen, Chet Jablonski, and John Bridson

Abstract: Reaction of $[\text{CpCo}(\text{C}_3\text{F}_7)(\text{I})(\text{L})]$, ($\text{L} = \text{PPh}_2\text{Me}$ (**1a**), PPhMe_2 (**1b**), PMe_3 (**1c**), and $\text{PPh}(\text{OMe})_2$ (**2**)), with $\text{PPh}(\text{OMe})_2$ affords diastereomeric Co- and P-chiral metallophosphinates $\text{CpCo}(\text{C}_3\text{F}_7)(\text{L})(\text{P}(\text{O})\text{Ph}(\text{OMe}))$, **4a,b,c** and **6**, respectively. The solid state structure and relative configuration of the lower R_f diastereomeric phosphinate $\text{CpCo}(\text{C}_3\text{F}_7)(\text{PPh}(\text{OMe})_2)(\text{P}(\text{O})\text{Ph}(\text{OMe}))$, **6-2**, was determined by X-ray diffraction. RR,SS -**6-2** crystallizes in the triclinic system with space group $P\bar{1}$ (no. 2), with $a = 12.928(4) \text{ \AA}$, $b = 14.683(4) \text{ \AA}$, $c = 7.666(2) \text{ \AA}$, $\alpha = 103.50(2)^\circ$, $\beta = 101.31(3)^\circ$, $\gamma = 109.50(2)^\circ$, $V = 1272.8(7) \text{ \AA}^3$, $Z = 2$, and $R = 0.036$ ($R_w = 0.030$) for 2867 reflections with $I > 3.00\sigma(I)$. $\text{CpCo}(\text{C}_3\text{F}_7)(\text{I})(\text{PPh}(\text{OMe})_2)$, **2**, reacts with PPh_2Me to yield the same Co- and P-chiral phosphinate products as obtained for the reaction of **1a** with $\text{PPh}(\text{OMe})_2$, albeit with different optical yields. The product stereochemistry is not accounted for by the established mechanism for transition metal Arbuzov-like dealkylations, which requires formation of a common, ionic intermediate $[\text{CpCo}(\text{C}_3\text{F}_7)(\text{PPh}_2\text{Me})(\text{PPh}(\text{OMe})_2)]^+$, **3**, via iodide substitution and subsequent nucleophilic attack at carbon. A parallel intramolecular dealkylation pathway is proposed to account for the results.

Key words: stereochemistry, mechanism, Arbuzov, Co(III) complex, chiral metal, X-ray

Résumé : La réaction du $[\text{CpCo}(\text{C}_3\text{F}_7)(\text{I})(\text{L})]$, ($\text{L} = \text{PPh}_2\text{Me}$ (**1a**), PPhMe_2 (**1b**), PMe_3 (**1c**) et $\text{PPh}(\text{OMe})_2$ (**2**)) avec du $\text{PPh}(\text{OMe})_2$ conduit aux métalophosphinates diastéréomériques Co- et P-chiraux $\text{CpCo}(\text{C}_3\text{F}_7)(\text{L})(\text{P}(\text{O})\text{Ph}(\text{OMe}))$ **4a,b,c** et **6** respectivement. Faisant appel à la diffraction des rayons X, on a déterminé les structures solides et les configurations relatives du phosphinate diastéréomère de R_f le plus faible, $\text{CpCo}(\text{C}_3\text{F}_7)(\text{PPh}(\text{OMe})_2)(\text{P}(\text{O})\text{Ph}(\text{OMe}))$, **6-2**. Le composé RR,SS -**6-2** cristallise dans le système triclinique, groupe d'espace $P\bar{1}$ (n° 2) avec $a = 12,928(4)$, $b = 14,683(4)$ et $c = 7,666(2) \text{ \AA}$, $\alpha = 103,50(2)^\circ$, $\beta = 101,31(3)^\circ$ et $\gamma = 109,50(2)^\circ$, $V = 1272,8(7) \text{ \AA}^3$, $Z = 2$ et $R = 0,036$ ($R_w = 0,030$) pour 2867 réflexions avec $I > 3,00\sigma(I)$. Le $\text{CpCo}(\text{C}_3\text{F}_7)(\text{I})(\text{PPh}(\text{OMe})_2)$, **2**, réagit avec du PPh_2Me pour conduire aux mêmes produits Co- et P-chiraux que ceux obtenus par réaction du composé **1a** avec du $\text{PPh}(\text{OMe})_2$; les rendements optiques sont toutefois différents. On ne peut pas expliquer la stéréochimie du produit en se basant sur le mécanisme établi pour les réactions de désalkylations de type Arbuzov des métaux de transition pour lesquels il est nécessaire de former un intermédiaire ionique commun, $[\text{CpCo}(\text{C}_3\text{F}_7)(\text{PPh}_2\text{Me})(\text{PPh}(\text{OMe})_2)]^+$, **3**, par le biais d'une substitution de l'iodure et d'une attaque nucléophile subséquente au niveau du carbone. Pour expliquer les résultats, on propose une voie réactionnelle parallèle de désalkylation intramoléculaire.

Mots clés : stéréochimie, mécanisme, Arbuzov, complexe de Co(III), métal chiral, rayon X.

[Traduit par la rédaction]

Introduction

Phosphites and phosphonites react readily with transition metal iodides to give metallophosphonates and -phosphinates, respectively (1, 2). Mechanistic studies have identified the predominant mechanism as a two-step sequence (cf. eq. [1]) that parallels the classic organophosphorus Arbuzov rearrangement (3–9). Initial halide substitution at the metal centre gives a cationic phosphite or phosphonite intermediate that can, in

favourable circumstance, be directly observed (1, 3–7, 9–12). Subsequent attack of halide ion at carbon occurs with C—O bond cleavage to displace the thermodynamically stable phosphoryl species. In the course of our studies of transition-metal-mediated Arbuzov chemistry as a platform for diastereoselective synthesis of P-chiral phosphinates from prochiral phosphonites, asymmetric Co(III) auxiliaries have been developed that afford P-chiral products with fair to good optical yields (2, 6, 13, 14). In this report we present evidence, derived from product distribution studies, which suggests that a novel, intramolecular dealkylation pathway competes with the accepted mechanism of eq. [1].

Results and discussion

Substitution and Arbuzov chemistry of **1** and **2**

Treatment of the iodo phosphine complexes $\eta^5\text{-CpCo}(\text{C}_3\text{F}_7)(\text{L})(\text{I})$ (**1a**, $\text{L} = \text{PPh}_2\text{Me}$; **1b**, $\text{L} = \text{PPhMe}_2$; **1c**, $\text{L} = \text{PMe}_3$ (**5**); **2**, $\text{L} = \text{PPh}(\text{OMe})_2$ (**14**)) with one equivalent of dimethyl phenylphosphonite in acetone at ambient temperature for 20 h affords a complex reaction mixture containing prod-

Received February 1, 1996.

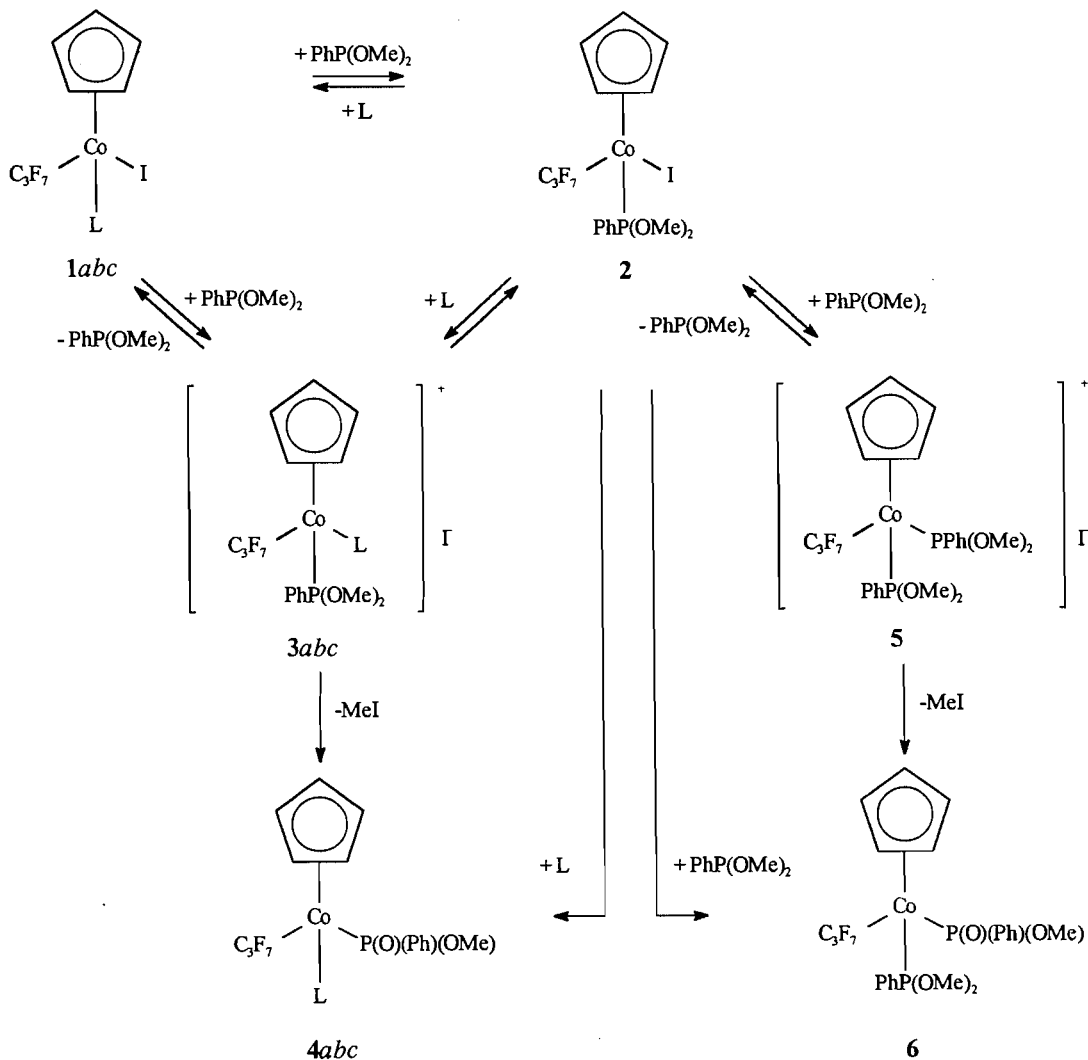
This paper is dedicated to Professor Howard C. Clark in recognition of his contributions to Canadian chemistry.

Z. Chen, C. Jablonski,¹ and J. Bridson. Department of Chemistry, Memorial University of Newfoundland, St. John's, NF A1B 3X7, Canada.

¹ Author to whom correspondence may be addressed. Telephone: (709) 737-8089. Fax: (709) 737-3702. E-mail: cjablons@morgan.ucs.mun.ca



Scheme 1.



ucts derived from simple phosphine substitution, halide substitution – Arbusov dealkylation, as well as combinations of both processes (cf. Scheme 1). Product structure was confirmed by comparison of NMR parameters with known compounds (**1c** (**5**) and **2** (**14**)) and by full analytical and spectroscopic characterization in the case of **1a** and **1b** (cf. Tables 1–3). Two diastereomeric pairs of enantiomers with characteristically different 1H NMR spectra were detected for all Co- and P-chiral metallophosphinates, η^5 -CpCo $^*(C_3F_7)(L)(P^*(O)Ph(OMe))$ **4a,b,c** and **6**.

Relative stereochemistry at chiral Co and P for the diastereomeric pairs of phosphine-substituted phosphinates **4a** and **4b**

was empirically assigned by comparison of relative chromatographic R_f values with those of crystallographically determined $RR;SS$ and $RS;SR$ -**4c** (**5**). We have found that $RR;SS$ diastereomers of this type consistently elute before the $RS;SR$ form on silica gel thin-layer chromatographic (TLC) plates. Thus the relative stereochemistry of the higher R_f diastereomers is assigned $RR;SS$ -**4a-1** and $RR;SS$ -**4b-1** and of the lower R_f diastereomers is $RS;SR$ -**4a-2** and $RS;SR$ -**4b-2**.

The relative stereochemistry of the lower R_f phosphonite-substituted product **6-2** was unambiguously established by single crystal X-ray diffraction study. The ORTEP representation of the molecular structure obtained (cf. Fig. 1) shows a

Table 1. Physical data for $\eta^5\text{-CpCo}^*(\text{C}_3\text{F}_7)(\text{L})(\text{X})$.

| Compound ^a | L, X | Formula | % yield | Analysis | | Relative config. | Melting point (°C) |
|-----------------------|---------------------------------------|---|---------|--------------------|--------------------|------------------|--------------------|
| | | | | % C found (calcd.) | % H found (calcd.) | | |
| 1a | PPh ₂ Me, I | C ₂₁ H ₁₈ F ₇ IPCo | 90.0 | 40.88 (40.67) | 3.03 (2.93) | | 155–160 |
| 1b | PPhMe ₂ , I | C ₁₆ H ₁₆ F ₇ IPCo | 86.6 | 34.53 (34.43) | 2.84 (2.89) | | 104–108 |
| 4a-1 | PPh ₂ Me, P(O)(OMe)(Ph) | C ₂₈ H ₂₆ F ₇ O ₂ P ₂ Co | 16.0 | 48.20 (51.87) | 4.04 (4.04) | <i>RR,SS</i> | 155–158 |
| 4a-2 | PPhMe ₂ , P(O)(OMe)(Ph) | C ₂₈ H ₂₆ F ₇ O ₂ P ₂ Co | 6.0 | — | — | <i>RS,SR</i> | 150–152 |
| 4b-1 | PPhMe ₂ , P(O)(OMe)(Ph) | C ₂₃ H ₂₄ F ₇ O ₂ P ₂ Co | 24.8 | 47.24 (47.12) | 4.10 (4.13) | <i>RR,SS</i> | 114–116 |
| 4b-2 | PPhMe ₂ , P(O)(OMe)(Ph) | C ₂₃ H ₂₄ F ₇ O ₂ P ₂ Co | 12.0 | — | — | <i>RS,SR</i> | 118–120 |
| 6-1 | P(O)(OMe)(Ph), P(O)(OMe)(Ph) | C ₂₃ H ₂₄ F ₇ O ₄ P ₂ Co | 34.9 | — | — | <i>RS,SR</i> | 149–151 |
| 6-2 | P(O)(OMe)(Ph), P(O)(OMe)(Ph) | C ₂₃ H ₂₄ F ₇ O ₄ P ₂ Co | 26.8 | 44.96 (44.68) | 4.05 (3.91) | <i>RR,SS</i> | 131–138 |

^aThe designation -1, -2 refers to high and low *R_f*, respectively.

Table 2. ¹H NMR data for $\eta^5\text{-CpCo}^*(\text{C}_3\text{F}_7)(\text{L})(\text{X})$.^a

| Compound | L, X | C ₆ H ₅ | Cp | OMe | PMe |
|-------------|------------------------------------|---|----------|---|----------------------------------|
| 1a | PPh ₂ Me, I | 7.83 (m), 7.64 (m), 7.47 (m) | 5.09 (s) | | 2.18 (d, 11) |
| 1b | PPhMe ₂ , I | 7.90 (m), 7.52 (m) | 4.91 (s) | | 2.12 (d, 11.1) 1.96 (d, 11.1) |
| 4a-1 | PPh ₂ Me, P(O)(OMe)(Ph) | 7.78 (m), 7.60 (m), 7.45 (m), 7.34 (m) | 5.06 (s) | 3.09 (d, 11.1) | 2.17 (d, 12.3) |
| 4a-2 | PPh ₂ Me, P(O)(OMe)(Ph) | 7.91 (m), 7.58 (m), 7.47 (m), 7.36 (m) | 4.87 (s) | 3.34 (d, 11.1) | 2.13 (d, 11.7) |
| 4b-1 | PPhMe ₂ , P(O)(OMe)(Ph) | 7.77 (m), 7.64 (m), 7.46 (m), 7.36 (m) | 4.86 (s) | 3.41 (d, 10.8) | 2.06 (d, 11.4) 1.90 (d, 11.4) |
| 4b-2 | PPhMe ₂ , P(O)(OMe)(Ph) | 7.92 (m), 7.79 (m), 7.48 (m), 7.40 (m) | 4.64 (s) | 3.42 (d, 11.1) | 2.01 (d, 11.4) 1.87 (d, 11.4) |
| 6-1 | P(O)(OMe)(Ph), P(O)(OMe)(Ph) | 7.73 (m), 7.50 (m), 7.33 (m) | 5.09 (s) | 3.83 (d, 10.8), 3.73 (d, 11.10), 3.41 (d, 10.8) | — |
| 6-2 | P(O)(OMe)(Ph), P(O)(OMe)(Ph) | 7.75 (m), 7.46 (m), 7.37 (m) | 4.98 (s) | 3.87 (d, 11.1), 3.81 (d, 10.5), 3.33 (d, 11.1) | — |

^a¹H NMR (300.1 MHz) chemical shifts in CDCl₃ relative to internal TMS; *J* values in Hz; m = multiplet, d = doublet.

typical pseudo-octahedral, three-legged piano-stool structure with average interligand bond angles (93.7°) approaching 90°. The phosphoryl P-atom is distorted from ideal tetrahedral geometry showing a moderate opening of the Co–P=O angle to 117.8° that is accommodated by a closing of the MeO–P–C(10) angle to 100.5°. A substantial multiple bond character (15) for the phosphoryl group is inferred from the P=O distance (1.487(3) Å), which is considerably shorter than the

P(1)—O(1) single bond length measured for **6-2** (1.625(3) Å) but comfortably in the normal range for free (15), P-coordinated (16, 17), or even P=O bridging (18) phosphoryl groups in a wide range of chemical environments (16, 17). The CIP ligand priority sequence Cp > PPh(OMe)₂ > P(O)(OMe)Ph > C₃F₇ for Co (19–21) and Co > OMe > O > Ph for P unambiguously fix the relative stereochemistry of **6-2** as *R_{Co}R_P*. CIP priority differences for phosphonite and phosphine show that

Table 3. ^{13}C and ^{31}P NMR data for $\eta^5\text{-CpCo}^*(\text{C}_3\text{F}_7)(\text{L})(\text{X})$.^a

| Compound | L, X | C_6H_5 | Cp | OMe | PMe | ^{31}P (PR ₃ , P—O) |
|----------|---------------------------------------|---|-------|---|-----------------|---|
| 1a | PPh ₂ Me, I | <i>i</i> : 137.56 (d, 43.3), 134.74 (d, 44.5) <i>o,m</i> : 132.65 (d, 7.8), 130.67 (d, 5.7), 128.49 (d, 8.7), 128.26 (d, 8.7) <i>p</i> : 132.80 | 87.75 | | 19.85 (d, 34.0) | 31.44, — |
| 1b | PPhMe ₂ , I | <i>i</i> : 139.02 (d, 43.2) <i>o,m</i> : 129.56 (d, 7.8), 128.85 (d, 8.3) <i>p</i> : 130.45 | 87.63 | | 16.74 (d, 39.6) | 19.02, — |
| 4a-1 | PPh ₂ Me, P(O)(OMe)(Ph) | <i>i</i> : 143.62 9(d, 49.5), 138.46 (d, 40.7), 136.93 (d, 50.1) <i>o,m</i> : 132.96 (d, 8.2), 130.59 (d, 10.3), 128.14 (d, 11.6), 127.40 (d, 12.4) <i>p</i> : 130.01, 129.64, 129.16 | 89.06 | 50.31 (d, 11.1) | 15.84 (d, 29.7) | |
| 4a-2 | PPh ₂ Me, P(O)(OMe)(Ph) | <i>i</i> : 141.29 (d, 52.5), 137.49 (d, 43.2), 136.71 (d, 49.6) <i>o,m</i> : 133.16 (d, 9.9), 132.27 (d, 8.8), 128.33 (d, 9.1), 127.75 (d, 10.9) <i>p</i> : 132.62, 130.31, 129.24 | 89.87 | 49.77 (d, 11.6) | 16.35 (d, 29.5) | |
| 4b-1 | PPhMe ₂ , P(O)(OMe)(Ph) | <i>i</i> : 143.33 (d, 49.6), 140.20 (d, 45.1), 132.24 (d, 51.32) <i>o,m</i> : 130.59 (d, 10.0), 130.06 (d, 7.9), 128.47 (d, 9.5), 127.56 (d, 11.2) <i>p</i> : 131.75, 129.62, 129.32 | 88.98 | 50.46 (d, 9.4) | 16.69 (d, 34.7) | |
| 4b-2 | PPhMe ₂ , P(O)(OMe)(Ph) | <i>i</i> : 143.99 (d, 53.1), 139.69, 132.72 (d, 39.6) <i>o,m</i> : 130.47 (d, 10.6), 130.20 (d, 7.7), 128.63 (d, 9.0), 127.91 (d, 11.4) <i>p</i> : 129.81, 129.45 | 90.03 | 49.72 (d, 14.4) | 17.77 (d, 30.6) | |
| 6-1 | P(O)(OMe)(Ph), P(O)(OMe)(Ph) | <i>i</i> : 143.73 (d, 58.2), 137.13 (d, 58.1) <i>o,m</i> : 131.25 (d, 10.6), 130.93 (d, 11.2), 128.05 (d, 10.4), 127.15 (d, 10.9) <i>p</i> : 131.00, 129.21 | 89.96 | 55.44 (d, 11.5), 54.26 (d, 10.4) | — | |
| 6-2 | P(O)(OMe)(Ph), P(O)(OMe)(Ph) | <i>i</i> : 144.48 (d, 58.3), 136.57 (d, 58.7) <i>o,m</i> : 131.25 (d, 10.6), 130.58 (d, 10.0), 127.83 (d, 12.9), 127.67 (d, 11.5) <i>p</i> : 130.93, 129.29 | 90.28 | 55.00 (d, 10.9), 54.74 (d, 10.0), 49.96 (d, 11.8) | — | |

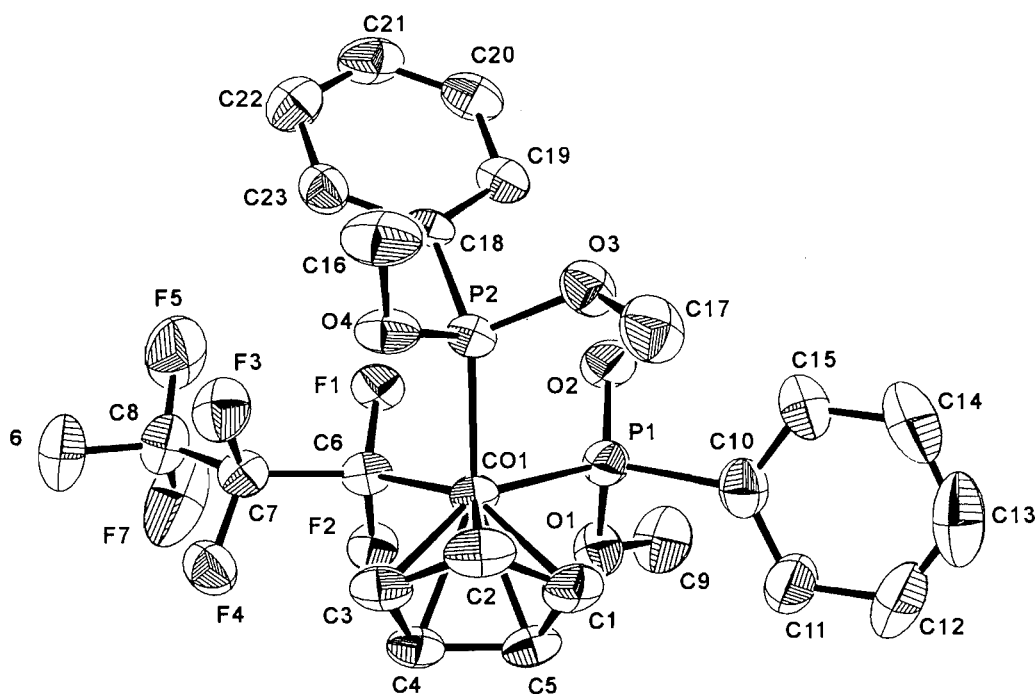
^a ^{13}C (75.47 MHz) chemical shifts in ppm relative to solvent CDCl_3 ; ^{31}P (121.5 MHz) chemical shifts in ppm relative to external 85% H_3PO_4 ; *J* values in Hz; d = doublet.

RR; *SS*-6-2 has the same relative stereochemistry as the lower *R_f* *RS*; *SR* diastereomers in the phosphine substituted series.

Product distribution was examined in detail for the case of reaction of **1a** with $\text{PPh}(\text{OMe})_2$. Careful preparative thick-layer chromatographic (PLC) isolation gives, in order of decreasing *R_f* values, unreacted **1a**, dark-green phosphonite complex $\eta^5\text{-CpCo}^*(\text{C}_3\text{F}_7)(\text{PPh}(\text{OMe})_2)(\text{I})$, **2**, two orange, phosphine-metallophosphonate diastereomers $\eta^5\text{-CpCo}^*(\text{C}_3\text{F}_7)(\text{PPh}_2\text{Me})\text{-}(\text{P}^*(\text{O})\text{Ph}(\text{OMe}))$, **4a-1,2**, followed by two light-orange phosphonite-metallophosphonate diastereomers (**14**) $\eta^5\text{-CpCo}^*(\text{C}_3\text{F}_7)(\text{PPh}(\text{OMe})_2)(\text{P}^*(\text{O})\text{Ph}(\text{OMe}))$, **6-1,2**. The iodo-phosphonite complex **2** is stable for months in the solid state or in acetone solution; however, it reacts readily in the presence of methyl-diphenylphosphine to afford the same sequence of products.

Product distribution was also monitored by ^1H NMR spectroscopy. We (**14**) as well as others (**22**) have observed that piano-stool $\text{Co}(\text{III})$ metallophosphonates such as **4** tend to be substitution inert, hence the phosphonite complexes **6-1** and **6-2** must derive from stepwise halide substitution and Arbuzov dealkylation of **2**. The observation that no phosphonite-containing products, **6**, were observed for the reaction of **1a** with dimethyl phenylphosphonite in the presence of excess PPh_2Me (mole ratio **1a**: $\text{PPh}(\text{OMe})_2$: PPh_2Me = 1:1:10) suggests a facile phosphine substitution that establishes the equilibrium $\text{1a} + \text{PPh}(\text{OMe})_2 \rightleftharpoons \text{2} + \text{PPh}_2\text{Me}$. Pre-equilibrium phosphine exchange was confirmed from observation of concentration/time curves vs. starting material ratios in acetone-*d*₆ solution. A labile species with $\delta_{\text{Cp}} = 5.60$ ppm was observed and tentatively assigned as the cationic intermediate **3a**; how-

Fig. 1. ORTEP plot of η^5 -CpCo⁺(C₃F₇)(PPh(OMe)₂)(P⁺(O)Ph(OMe)), 6-2.



ever, we are unable to unequivocally distinguish whether formation of **4** proceeds by direct phosphine exchange ($2 \rightarrow 4$) and (or) via the proposed cationic intermediate **3a** ($1,2 \rightarrow 3 \rightarrow 4$). Nevertheless, all directly observed products follow directly from consideration of Scheme 1.

Stereochemistry and optical yields

If cationic $[\eta^5\text{-CpCo}(\text{C}_3\text{F}_7)(\text{PPh}_2\text{Me})(\text{PPh}(\text{OMe})_2)]^+\text{I}^-$, **3a**, is the unique intermediate for transition metal Arbuzov dealkylation (Scheme 1), treatment of the iodo-phosphine complex $\eta^5\text{-CpCo}(\text{C}_3\text{F}_7)(\text{PPh}_2\text{Me})(\text{I})$, **1a**, with dimethyl phenylphosphonite or of the iodo-phosphonite complex $\eta^5\text{-CpCo}^+(\text{C}_3\text{F}_7)(\text{PPh}(\text{OMe})_2)(\text{I})$, **2**, with methyl diphenylphosphine is expected to produce identical optical yields of P-chiral metallophosphinate product, **4**. In that event %de is fully determined by $\Delta\Delta G^\ddagger$ for iodide attack at the diastereotopic methoxy groups of intermediate **3a** as shown in Scheme 1. In contrast with this hypothesis, we find that the optical yield of phosphinate $\eta^5\text{-CpCo}(\text{C}_3\text{F}_7)(\text{PPh}_2\text{Me})(\text{P}(\text{O})\text{-Ph}(\text{OMe}))$ (%de = $100 \times ([4a-1] - [4a-2]) / ([4a-1] + [4a-2])$) is sensitive to reactant composition in acetone (cf. Table 4). Table 4 shows the dependence of optical yield on reactant composition as determined by integration of ¹H NMR spectra in the Cp region. Relative stereochemistry for the Co- and P-chiral metallophosphinates **4a** and **4b** was assigned by comparison of TLC *R_f* values with that of crystallographically determined **4c**. (5). Reaction of **1a** with PPh(OMe)₂ resulted in increased optical yield for **4a-1**, **4a-2** compared with reaction of **2** with PPh₂Me (cf. Table 4 entries 1 and 3). The product distribution studies are inconsistent with the formation of a common intermediate and therefore imply the presence of a parallel reaction channel with a different optical yield. We propose a competing,

intramolecular pathway, which is possible only for the iodo-phosphonite **2**.

There is ample literature precedent that establishes that intramolecular alkyl migrations can lead to metallophosphonates (23–25). We therefore propose an intramolecular attack of iodide at carbon, concerted with associative nucleophilic attack at the metal by PPh₂Me. Expulsion of MeI from **2** gives the metallophosphinate **4a-1**, **4a-2** in a single step as illustrated in Scheme 2. Optical yield for **4a** formation via the intramolecular pathway is then a function of $\Delta\Delta G^\ddagger$ (intramolecular) rather than $\Delta\Delta G^\ddagger$ (intermolecular) for iodide attack at diastereotopic OMe (cf. Scheme 2). Optical yields will then reflect the position of the equilibrium connecting the starting materials **1** and **2**. In the presence of excess PPh₂Me the equilibrium $1a + \text{PPh}(\text{OMe})_2 \rightleftharpoons 2 + \text{PPh}_2\text{Me}$ shifts to the left and effectively shuts off the intramolecular route. Under these conditions (cf. Table 4, entry 6) the intermolecular sequence $1a \rightarrow 3a \rightarrow 4a$ provides the dominant route to phosphinate product. If our interpretation is correct, higher %de in the presence of excess PPh₂Me can be interpreted as less efficient optical induction for the intramolecular vs. intermolecular pathway. Accordingly, the lowest optical yields were measured in methanol solvent (cf. Table 4, entry 8) since hydrogen bonding limits iodide nucleophilicity and the intramolecular pathway operates exclusively (cf. discussion below).

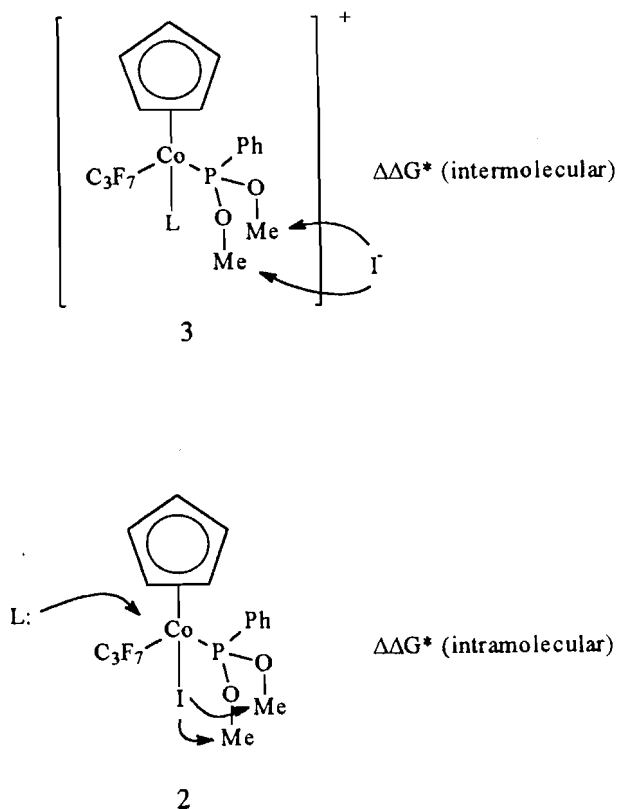
Attempts to further test for the proposed intramolecular Arbuzov reaction mechanism by reacting $[\eta^5\text{-CpCo}(\text{C}_3\text{F}_7)(\text{PPh}_2\text{Me})(\text{PPh}(\text{OMe})_2)]^+\text{SbF}_6^-$, prepared by iodide abstraction of **2** followed by in situ treatment with PPh₂Me, with NaI in acetone failed. Reaction under these conditions resulted in nucleophilic attack of iodide on cobalt rather than carbon. The

Table 4. Product distribution vs. reactant composition for Scheme 1.

| Entry no. | Reactant composition (mol ratio) | Solvent | Yield (mol %) ^a | | | |
|-----------|--|---------------------------|----------------------------|-------|---|----------------------------------|
| | | | 1a | 2 | RR,SS-4a-1/ RS,SR-4a-2 (%de) ^b | RS,SR-6-1/ RR,SS-6-2 (%de) |
| 1 | 1a:PPh(OMe) ₂ = 1:1 | Acetone | 53.4 | 16.4 | 16.0/6.0 (46) | 4.9/3.3 (19.5) |
| 2 | 1a:PPh(OMe) ₂ = 1:3 | Acetone | Trace | Trace | 3.3/1.1 (50) | 46.7/41.6 (5.8) |
| 3 | 2:PPh ₂ Me = 1:1 | Acetone | 40.6 | 4.5 | 32.1/14.3 (38.2) | 5.3/3.2 (25) |
| 4 | 2:PPh ₂ Me = 1:1 | Benzene | 69.9 | 21.8 | 2.5/1.1 (38.9) | 2.8/2.0 (16.7) |
| 5 | 2:1a:PPh ₂ Me = 1:2:1 | Acetone | 74.9 | 11.6 | 9.6/3.9 (42.2) | Trace |
| 6 | 1a:PPh(OMe) ₂ :PPh ₂ Me = 1:1:10 | Acetone | 51.8 | Trace | 37.9/10.3 (57.3) | Trace |
| 7 | 1a:PPh(OMe) ₂ :PPh ₂ Me = 1:1:10 | Acetone:methanol = 3:2 | >90 | Trace | Trace | Trace |
| 8 | 2:PPh ₂ Me = 1:1 | Acetone:methanol = 3:2 | 56.9 | 12.4 | 12.6/7.4 (26.2) | 6.5/4.3 (20.4) |

^aDetermined by ¹H NMR integration of the η⁵-Cp region.

^b%de = (|[RR,SS]-[RS,SR]|)/([RR,SS]+[RS,SR]) × 100.

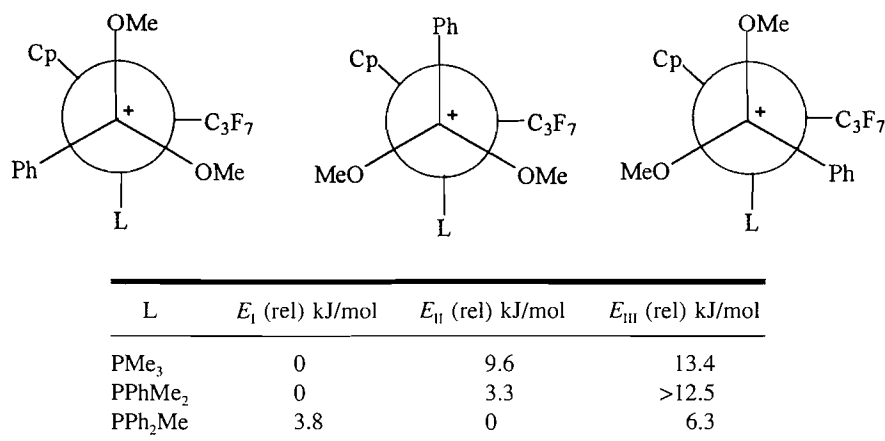
Scheme 2.

iodo complexes, resulting from phosphonite/phosphine substitution, were isolated in a 14.5:1 ratio in > 90% chemical yield.

Brunner's early studies (26) of coordinatively saturated, pseudo-tetrahedral, piano-stool complexes elegantly established dissociative substitution with dominant retention of configuration at chiral metal. Fewer examples of associative activation have been identified (27–30). The latter require an ancillary ligand capable of removing an electron pair in order to avoid formation of high-energy 20 e⁻ species. Established cases involve hapticity decreases (η⁵→η³ "ring slippage" (27)) of indenyl or cyclopentadienyl or linear→bent NO isomerization (31). In a relevant study Landon and Brill (3) reported second-order kinetics for the Arbusov rearrangement of η⁵-CpCo(dppe)I with P(OMe)₃ and steric inhibition for the increased bite-angle ligand dppe (1,3-bis(diphenylphosphino)propane), implying an associative reaction. The stereochemical consequences pursuant to the presence of a prochiral phosphonite in the present study allow detection of an otherwise masked reaction mechanism.

Solvent effects

Solvent effects also support the proposed intramolecular Arbusov dealkylation. Free iodide ion is strongly solvated in protonic solvents and is considerably less nucleophilic (6), hence attack at carbon required for Arbusov dealkylation is inhibited. Complex 1a reacts with PPh(OMe)₂ in the presence of excess PPh₂Me via initial displacement of iodide; however, the second step is effectively blocked in methanol and Arbusov dealkylation does not proceed readily (cf. Table 4, entry

Fig. 2. GMMX determined conformational energies for **3**.

7). If other reaction pathways were available under these conditions, **4a-1**, and **4a-2** would still be formed.

Strikingly different results were obtained when the reaction was carried out starting with **2** in the methanol-*d*₄ (cf. Table 4, entry 8). Addition of one equivalent of PPh₂Me resulted in the formation of four Cp peaks in the ¹H NMR spectrum assigned to **1a**, **2**, **4a-1**, and **4a-2**. Arbusov dealkylation occurs readily from **2** even when the two-step pathway **2**→**3a**→**4a** is blocked in protonic media. Since iodide is non-nucleophilic under these conditions, iodide attack at OCH₃ cannot occur from outside the coordination sphere. In contrast, protonic solvent is expected to have little effect on a concerted mechanism involving **3** that avoids formation of free iodide. Optical yields in this experiment are determined exclusively by the intramolecular mechanism and decreased to %de = 28, consistent with a decreased optical induction in the intramolecular route.

It is reasonable to expect that low dielectric media will inhibit iodide substitution since the process involves substantial charge separation. Indeed (cf. Table 4, entry 4) we find that the optical yield for the reaction of **2** with PPh₂Me drops as the solvent changes from acetone ($\epsilon = 20$, %de = 32) to benzene ($\epsilon = 4$, %de = 15).

Ligand sphere effects on optical yield

$\Delta\Delta G^\ddagger$ for attack of iodide at the diastereotopic phosphonite methoxy groups will of course determine optical yield. Previous studies of Co→P chiral induction for **1**→**4** (L = PPh₂NH(C⁺H(Me)Ph)) identified (2, 13, 14) intramolecular N—H⋯O=P hydrogen bonding as a pivotal parameter for Co→P chiral induction. We were therefore surprised to find that optical yields measured for **1**→**4** (L = phosphine, phosphonite), which cannot reduce the number of low-energy conformers by intramolecular hydrogen bonding, were in some cases superior. Measured optical yields for **1**→**4** decreased along the series L = PPh₂Me (40%) < PPhMe₂ (33%) < PMe₃ (18%). It was of interest to determine the effect of ligand steric requirements on the efficacy of Co→P optical induction.

Molecular mechanics global minimum conformational searches for the intermediates **3a-c** were carried out using the GMMX algorithm (32) with the assumption that insight relevant to diastereoselection in the transition state for intermolecular dealkylation might be provided. Starting structures for the

conformations **3**, obtained from model compounds derived from crystallographic data, were minimized using the MMX (33) force field, which has been shown to be appropriate for related piano-stool molecules (34, 35). GMMX searches of conformational space used a combined Monte Carlo internal – Cartesian randomization protocol that examined rotations about all specified bonds with less than 3-fold symmetry. Conformations meeting energy criteria were then MMX minimized, checked for redundancy, and retained subsequent to a final energy assessment. Surviving conformations within a 12.5 kJ/mol band containing the lowest energy structure were retained. Further cycles removed/re-added hydrogen atoms in calculated positions and minimized in order to dislodge structures from saddle points. Finally, the surviving conformations were checked for redundancy and energy criteria. The process was continued until no further conformations were lost.

The GMMX conformational searches identified three staggered Co-P(OMe)₂Ph rotamers for the intermediate **3a,b,c**. Figure 2 shows Newman projections along with the calculated relative MMX energies. Literature evidence (36, 37) strongly suggests that the region between the almost 90° L-Co-C₃F₇ is the least sterically accessible for pseudo-octahedral piano stools. The GMMX calculations concur, and rotamers I and II, which place the least sterically demanding group (OMe) in that region, are always most stable. Face/edge Cp–Ph interactions (38–40) may also contribute to the relative stability of rotamers I and II. Differences are small; however, the relative increase in the energy of rotamer I with respect to II as phenyl groups accumulate on the phosphine donor L can be traced to increasing Ph–L steric interactions.

Curtin–Hammett restrictions (41) preclude a direct relation between conformer population and optical yield, however, based on the GMMX calculations described above, a case can be made for the direction of chiral induction and ligand sphere effects on the measured %de for **1**→**3**→**4**. It is clear that the critical step for chiral induction occurs on attack of iodide at the diastereotopic OMe groups of **3**, which displaces the phosphoryl product. We have previously established a preference for a dominant *anticlinal* Cp–Co–P=O conformation (2, 13, 14, 42, 43) in piano-stool metallophosphonate and metallophosphinate complexes. Assumption of significant product-like character in the transition state predicts a preference for

attack at the *anticlinal* Cp-Co-P-OMe, and conformer II (R_{Co} configuration shown in Fig. 2) is then correctly linked to the major product ($R_{Co}R_P$). Optical yields will then parallel the II/I ratio, which increases along the series PMe_3 (18%de) < $PPhMe_2$ (33%de) < PPh_2Me (40%de).

Experimental

General

All manipulations were performed under a dry nitrogen atmosphere using standard Schlenk techniques. Nitrogen was purified by passing through a series of columns containing granular phosphorus pentoxide, 3A molecular sieves, and BASF DEOX catalyst (100°C). Acetone, methanol, and methylene chloride were distilled from activated 4A molecular sieves. Reactions were monitored by analytical thin-layer chromatography (precoated TLC plates, silica gel F-254, Merck). NMR spectra were recorded on a General Electric GN300-NB spectrometer operating at a proton frequency of 300.1 MHz. Preparative thick-layer chromatographic (PLC) purification was carried out using a Chromatotron (Harrison Associates) with 1–2 mm thick silica gel₆₀PF₂₅₄(Merck) adsorbent. The compounds $CpCo(C_3F_7)(CO)(I)$ (44), **1c** (5), and **2** (14) were prepared using the established procedures. Commercial samples of dimethyl phenylphosphonite, diphenylmethylphosphine, dimethylphenylphosphine, trimethylphosphine, $AgSbF_6$, and perfluoropropyl iodide (Aldrich) were used as received. Melting points were measured in sealed, nitrogen-filled capillaries and are uncorrected. C, H analyses were provided by Canadian Microanalytical Service Inc., Delta, B.C.

Preparation of $\eta^5-CpCo^*(C_3F_7)(PPh_2Me)(I)$ (**1a**) and $\eta^5-CpCo^*(C_3F_7)(PPhMe_2)(I)$ (**1b**).

PPh_2Me (90.1 mg, 0.450 mmol) was added dropwise to a stirred 25 mL, black, CH_2Cl_2 solution of $\eta^5-CpCo^*(C_3F_7)(CO)(I)$ (197.4 mg, 0.4407 mmol) contained in a 100 mL Schlenk flask and stirred at ambient temperature (20°C) for 12 h. Removal of volatiles under water aspirator followed by oil pump vacuum overnight left a dark green solid, which was purified by thick-layer radial PLC on silica gel (CH_2Cl_2) to give **1a** (245.9 mg, 0.3966 mmol, 90.0%). **1b** was prepared in 86.6% yield from $\eta^5-CpCo^*(C_3F_7)(CO)(I)$ and $PPhMe_2$ in an analogous manner. Physical, analytical, and spectroscopic data for **1a,b** are presented in Tables 1–3.

Reaction of $\eta^5-CpCo^*(C_3F_7)(PPh_2Me)(I)$ (**1a**) with $PPh(OMe)_2$ in acetone

$\eta^5-CpCo^*(C_3F_7)(PPh_2Me)(I)$ (134.0 mg, 0.2161 mmol), $PPh(OMe)_2$ (38.0 mg, 0.2188 mmol), and acetone (25 mL) were mixed in a 50 mL Schlenk flask and stirred at ambient temperature (20°C) for 24 h. Removal of volatiles under water aspirator followed by oil pump vacuum overnight left a dark-green solid, which was purified by PLC on silica gel. Elution with CH_2Cl_2 separated (in order of decreasing R_f values) a dark-green zone containing **1a** (71.6 mg, 0.115 mmol) and **2** (20.9 mg, 0.0354 mmol). Continued elution with acetone separated two orange zones containing **4a-1**, **4a-2** (**4a-1**: 22.4 mg, 0.0346 mmol; **4a-2**: 8.4 mg, 0.013 mmol), followed by two light-orange zones containing **6-1**, **6-2** (**6-1**: 7.6 mg 0.012 mmol; **6-2**: 3.1 mg 0.0050 mmol). Physical, analytical, and spectroscopic data for **4a-1,2** are presented in Tables 1–3.

Table 5. Positional parameters^a and $B(eq)$ for **6-2**.

| Atom | x | y | z | $B(eq)$ |
|-------|------------|------------|------------|---------|
| Co(1) | 0.86631(5) | 0.29330(4) | 0.09365(7) | 2.40(2) |
| P(1) | 0.7104(1) | 0.28599(8) | -0.1076(1) | 2.95(4) |
| P(2) | 0.7909(1) | 0.13075(8) | 0.0634(1) | 2.65(3) |
| F(1) | 0.8736(2) | 0.1979(2) | -0.2712(3) | 3.19(7) |
| F(2) | 0.9669(2) | 0.3631(2) | -0.1680(3) | 3.27(8) |
| F(3) | 1.0482(2) | 0.1915(2) | 0.0153(3) | 4.6(1) |
| F(4) | 1.1412(2) | 0.3528(2) | 0.0618(3) | 4.6(1) |
| F(5) | 1.0409(3) | 0.1502(3) | -0.3496(4) | 7.9(1) |
| F(6) | 1.2075(2) | 0.2376(2) | -0.1636(4) | 5.8(1) |
| F(7) | 1.1201(3) | 0.3080(3) | -0.3146(4) | 7.9(2) |
| O(1) | 0.7527(2) | 0.3853(2) | -0.1762(4) | 3.6(1) |
| O(2) | 0.6437(2) | 0.1908(2) | -0.2704(4) | 4.1(1) |
| O(3) | 0.6686(2) | 0.0891(2) | 0.0997(4) | 3.8(1) |
| O(4) | 0.8767(2) | 0.1111(2) | 0.2178(4) | 3.4(1) |
| C(1) | 0.8418(4) | 0.3768(3) | 0.3323(5) | 3.6(1) |
| C(2) | 0.9123(4) | 0.3273(3) | 0.3888(5) | 3.7(2) |
| C(3) | 1.0123(4) | 0.3621(3) | 0.3351(5) | 3.4(1) |
| C(4) | 1.0044(4) | 0.4355(3) | 0.2452(5) | 3.2(1) |
| C(5) | 0.8988(4) | 0.4438(3) | 0.2430(5) | 3.3(1) |
| C(6) | 0.9399(3) | 0.2786(3) | -0.1069(5) | 2.6(1) |
| C(7) | 1.0567(3) | 0.2660(3) | -0.0633(6) | 3.0(1) |
| C(8) | 1.1058(4) | 0.2405(4) | -0.2265(7) | 4.1(2) |
| C(9) | 0.6711(4) | 0.3929(4) | -0.3224(7) | 5.1(2) |
| C(10) | 0.6082(4) | 0.3133(4) | 0.0116(6) | 3.8(2) |
| C(11) | 0.6180(4) | 0.4117(4) | 0.0951(7) | 4.9(2) |
| C(12) | 0.5393(5) | 0.4279(5) | 0.1864(8) | 6.6(3) |
| C(13) | 0.4520(6) | 0.3463(7) | 0.1949(9) | 7.3(3) |
| C(14) | 0.4400(4) | 0.2492(5) | 0.1098(8) | 6.3(2) |
| C(15) | 0.5168(4) | 0.2320(4) | 0.0177(7) | 4.7(2) |
| C(16) | 0.8434(4) | 0.0169(3) | 0.2639(6) | 5.0(2) |
| C(17) | 0.6508(4) | 0.1241(4) | 0.2800(7) | 5.2(2) |
| C(18) | 0.7575(3) | 0.0270(3) | -0.1505(5) | 2.7(1) |
| C(19) | 0.6529(3) | -0.0114(3) | -0.2911(6) | 3.4(1) |
| C(20) | 0.6257(4) | -0.0947(3) | -0.4479(6) | 4.2(2) |
| C(21) | 0.7018(5) | -0.1397(3) | -0.4646(6) | 4.4(2) |
| C(22) | 0.8062(4) | -0.1032(4) | -0.3287(7) | 4.6(2) |
| C(23) | 0.8335(3) | -0.0195(3) | -0.1728(6) | 3.6(1) |

^aEstimated standard deviations in the least significant figure are given in parentheses.

Reaction of $\eta^5-CpCo^*(C_3F_7)(PPhMe_2)(I)$ (**1b**) with $PPh(OMe)_2$ in acetone

$\eta^5-CpCo^*(C_3F_7)(PPhMe_2)(I)$ (41.3 mg, 0.0749 mmol), $PPh(OMe)_2$ (20.8 mg, 0.122 mmol), and acetone (25 mL) were mixed in a 50 mL Schlenk flask and stirred at 50°C for 12 h. Removal of volatiles under water aspirator followed by oil pump vacuum overnight left a dark-green solid, which was purified by PLC on silica gel. Elution with CH_2Cl_2 separated (in order of decreasing R_f values) a dark-green zone containing **1b** and **2** (17.6 mg). Continued elution with acetone separated two orange zones containing **4b-1**, **4b-2** (**4b-1**: 10.9 mg, 0.0186 mmol; **4b-2**: 5.3 mg, 0.0090 mmol). Physical, analytical, and spectroscopic data for **4b-1,2** are presented in Tables 1–3.

Table 6. Selected intramolecular distances^a and angles for **6-2**.

| Atom | Atom | Distance (Å) | Atom | Atom | Distance (Å) |
|-------|-------|--------------|------|-------|--------------|
| Co(1) | P(1) | 2.239(2) | O(3) | C(17) | 1.450(5) |
| Co(1) | P(2) | 2.191(1) | O(4) | C(16) | 1.453(5) |
| Co(1) | C(1) | 2.095(4) | C(1) | C(2) | 1.407(6) |
| Co(1) | C(2) | 2.114(4) | C(1) | C(5) | 1.416(5) |
| Co(1) | C(3) | 2.120(4) | C(2) | C(3) | 1.403(6) |
| Co(1) | C(4) | 2.112(4) | C(3) | C(4) | 1.429(5) |
| Co(1) | C(5) | 2.093(4) | C(4) | C(5) | 1.408(6) |
| Co(1) | C(6) | 1.967(4) | C(6) | C(7) | 1.563(5) |
| P(1) | O(1) | 1.625(3) | C(7) | C(8) | 1.537(6) |
| P(1) | O(2) | 1.487(3) | | | |
| P(1) | C(10) | 1.843(4) | | | |
| P(2) | O(3) | 1.599(3) | | | |
| P(2) | O(4) | 1.603(3) | | | |
| P(2) | C(18) | 1.820(4) | | | |

| Atom | Atom | Atom | Angle (°) | Atom | Atom | Atom | Angle (°) |
|-------|-------|-------|-----------|-------|------|-------|-----------|
| P(1) | Co(1) | P(2) | 93.68(5) | O(2) | P(1) | C(10) | 107.3(2) |
| P(1) | Co(1) | C(6) | 90.9(1) | Co(1) | P(2) | O(4) | 107.3(1) |
| P(2) | Co(1) | C(6) | 96.5(1) | Co(1) | P(2) | C(18) | 124.7(1) |
| Co(1) | P(1) | O(1) | 106.3(1) | O(3) | P(2) | O(4) | 105.4(2) |
| Co(1) | P(2) | O(3) | 116.8(1) | O(3) | P(2) | C(18) | 97.0(2) |
| Co(1) | P(1) | O(2) | 117.8(1) | O(4) | P(2) | C(18) | 103.7(2) |
| Co(1) | P(1) | C(10) | 112.2(1) | P(1) | O(1) | C(9) | 117.5(3) |
| O(1) | P(1) | O(2) | 111.4(2) | P(2) | O(3) | C(17) | 123.0(3) |
| O(1) | P(1) | C(10) | 100.5(2) | P(2) | O(4) | C(16) | 122.1(3) |

^aEstimated standard deviations in the least significant figure are given in Parenthesis.

Reaction of $\eta^5\text{-CpCo}^*(\text{C}_3\text{F}_7)(\text{PPh}(\text{OMe})_2)(\text{I})$ **2** with PPh_2Me in acetone

$\eta^5\text{-CpCo}^*(\text{C}_3\text{F}_7)(\text{PPh}(\text{OMe})_2)(\text{I})$ (147.0 mg, 0.2491 mmol), PPh_2Me (51.0 mg, 0.255 mmol), and acetone (25 mL) were mixed in a 50 mL Schlenk flask and stirred at ambient temperature (20°C) for 24 h. Removal of volatiles under water aspirator followed by oil pump vacuum overnight left a dark-green solid, which was purified by PLC on silica gel. Elution with CH_2Cl_2 separated (in order of decreasing R_f values) a dark-green zone containing **1a** (62.1 mg, 0.100 mmol) and **2** (6.6 mg, 0.011 mmol). Continued elution with acetone separated two orange zones containing **4a-1**, **4a-2** (**4a-1**: 45.1 mg, 0.0696 mmol; **4a-2**: 21.0 mg, 0.0324 mmol), followed by two light-orange zones containing **6-1**, **6-2** (**6-1**: 7.9 mg 0.013 mmol; **6-2**: 4.4 mg 0.0071 mmol).

Reaction of $\eta^5\text{-CpCo}^*(\text{C}_3\text{F}_7)(\text{PPh}(\text{OMe})_2)(\text{I})$ **2** with AgSbF_6 following with PPh_2Me and then NaI in acetone

A 10 mL colourless, acetone solution of AgSbF_6 (29.1 mg, 0.0847 mmol) was added dropwise with stirring into a 20 mL dark-green acetone solution of $\eta^5\text{-CpCo}^*(\text{C}_3\text{F}_7)(\text{PPh}(\text{OMe})_2)(\text{I})$ (44.0 mg, 0.0755 mmol) contained in a 50 mL Schlenk flask at ambient temperature (20°C). A white precipitate of AgI formed. Dropwise addition of PPh_2Me (16.6 mg, 0.0829 mmol) resulted in the formation of a brown solution. Treatment of the solution with NaI (22.8 mg, 0.1521 mmol) gave an immediate colour change to deep green. Removal of volatiles under water aspirator pressure followed by oil pump

vacuum overnight left a dark-green solid. ^1H NMR analysis (CDCl_3) of the residue in cyclopentadienyl region showed two resonances corresponding to **1a** ($\delta = 5.09$ ppm, 75.0%) and **2** ($\delta = 5.19$ ppm, 17.2%). The phosphinate complexes **4a-1**, **4a-2** were not detected.

NMR tube reaction of $\eta^5\text{-CpCo}^*(\text{PPh}(\text{OMe})_2)(\text{I})$, **2**, with PPh_2Me in acetone- d_6

A 5 mm NMR tube was charged with $\eta^5\text{-CpCo}^*(\text{C}_3\text{F}_7)(\text{PPh}(\text{OMe})_2)(\text{I})$ (13.44 mg, 0.02276 mmol), PPh_2Me (4.78 mg, 0.0239 mmol), and acetone- d_6 (0.86 mL) and capped with a septum. The sample was equilibrated at ambient temperature (20°C) for 24 h. The ^1H NMR spectrum showed **1a** ($\delta = 5.25$ ppm, 45.4%), **2** ($\delta = 5.37$ ppm, 5.5%), **4a-1** ($\delta = 5.20$ ppm, 23.5%), **4a-2** ($\delta = 4.95$ ppm, 8.4%), **6-1** ($\delta = 5.18$ ppm, 7.1%), **6-2** ($\delta = 4.98$ ppm, 6.3%), respectively. A parallel reaction was carried out for $\text{CpCo}^*(\text{C}_3\text{F}_7)(\text{PPh}(\text{OMe})_2)(\text{I})$ with PPh_2Me , resulting in **1a** ($\delta = 5.25$ ppm, 30.1%), **2** ($\delta = 5.37$ ppm, 4.2%), **4a-1** ($\delta = 5.20$ ppm, 26.9%), **4a-2** ($\delta = 4.95$ ppm, 13.3%), **6-1** ($\delta = 5.18$ ppm, 7.6%), **6-2** ($\delta = 4.98$ ppm, 8.0%), respectively.

Reaction of $\eta^5\text{-CpCo}^*(\text{C}_3\text{F}_7)(\text{PPh}_2\text{Me})(\text{I})$, **1a**, with

$\text{PPh}(\text{OMe})_2$ in acetone in the presence of excess PPh_2Me $\eta^5\text{-CpCo}^*(\text{C}_3\text{F}_7)(\text{PPh}_2\text{Me})(\text{I})$ (27.0 mg, 0.0435 mmol), $\text{PPh}(\text{OMe})_2$ (7.6 mg, 0.045 mmol), and PPh_2Me (95.8 mg, 0.478 mmol) were mixed in 10 mL of acetone in a 50 mL Schlenk flask and stirred at ambient temperature (20°C) for 24

Table 7. Summary of crystallographic data for 6-2.

| | |
|--|---|
| Formula | C ₂₃ H ₂₄ O ₄ F ₇ P ₂ Co |
| FW (g/mol) | 618.31 |
| Crystal habit | Orange column |
| Crystal size (mm) | 0.45 × 0.12 × 0.10 |
| Crystal system | Triclinic |
| Lattice parameters | |
| <i>a</i> (Å) | 12.928(4) |
| <i>b</i> (Å) | 14.683(4) |
| <i>c</i> (Å) | 7.666(2) |
| α (°) | 103.5(2) |
| β (°) | 101.31(3) |
| γ (°) | 109.50(2) |
| <i>V</i> (Å ³) | 1272.8(4) |
| Space group | <i>P</i> $\bar{1}$ (no. 2) |
| <i>Z</i> | 2 |
| <i>D</i> _{calcd} (g/cm ³) | 1.613 |
| <i>F</i> ₀₀₀ | 628 |
| μ _(MoKα) (cm ⁻¹) | 8.73 |
| Scan width (°) | 1.47 + 0.30 tan θ |
| 2θ _{max} (°) | 50.0 |
| No. of reflections measured | |
| Total | 4682 |
| Unique | 4469 |
| <i>R</i> _{int} | 0.027 |
| Corrections ^a | Lorentz-polarization absorption |
| Trans.factors: | 0.95-1.00 |
| Secondary extinction coeff. | 0.25290 × 10 ⁻⁶ |
| Function minimized | Σ <i>w</i> (<i>F</i> _o - <i>F</i> _c) ² |
| Least-squares weights | 4 <i>F</i> _o ² /σ ² (<i>F</i> _o ²) |
| <i>p</i> -Factor | 0.01 |
| Anomalous dispersion | All non-hydrogen atoms |
| No. of observations (<i>I</i> > 2.00σ(<i>I</i>)) | 2867 |
| No. of variables | 335 |
| Reflection/parameter ratio | 8.56 |
| <i>R</i> ^b | 0.036 |
| <i>R</i> _w ^c | 0.030 |
| Goodness of fit indicator ^d | 1.45 |
| Max shift/error in final cycle | 0.71 |
| Δ <i>p</i> Final (max/min) (e ⁻ /Å ³) | 0.33/ - 0.25 |

^acf. ref. 46.^b $R = \sum (|F_o| - |F_c|) / \sum |F_o|$.^c $R_w = [(\sum w(|F_o| - |F_c|)^2) / \sum w F_o^2]^{1/2}$.^dGOF = (Σ(|*F*_o| - |*F*_c|)/σ)/(*n* - *m*) where *n* = no. of reflections, *m* = no. of variables, and σ² = variance of (|*F*_o| - |*F*_c|).

h. Removal of volatiles under water aspirator followed by oil pump vacuum overnight left a dark-green solid. ¹H NMR analysis in CDCl₃ showed three cyclopentadienyl resonances corresponding to **1a** (δ = 5.09 ppm, 51.4%), **4a-1** (δ = 5.06 ppm, 40.1%), and **4a-2** (δ = 4.87 ppm, 10.8%).

Reaction of η⁵-CpCo*(C₃F₇)(PPh₂Me)(I), **1a**, with

PPh(OMe)₂ in acetone/methanol

η⁵-CpCo*(C₃F₇)(PPh₂Me)(I) **1a** (21.8 mg, 0.0352 mmol), PPh(OMe)₂ (6.0 mg, 0.035 mmol), and PPh₂Me (69.1 mg, 0.345 mmol) were combined in 3/2 (v/v) acetone/methanol (10 mL) in a 50 mL Schlenk flask at ambient temperature (20°C) and stirred for 24 h. The ¹H NMR spectrum of the crude product showed only one cyclopentadienyl resonance (δ = 5.09

ppm) assigned to the starting material **1a** in CDCl₃. A similar reaction starting with η⁵-CpCo(C₃F₇)(PPh(OMe)₂)(I) **2** (43.3 mg, 0.0734 mmol) and PPh₂Me (14.7 mg, 0.0735 mmol) in 3/2 (v/v) acetone/methanol gave **1a** (δ = 5.09 ppm, 50.7%), **2** (δ = 5.19 ppm, 11.0%), **4a-1** (δ = 5.06 ppm, 11.25%), **4a-2** (δ = 4.87 ppm, 6.6%), respectively.

Reaction of η⁵-CpCo*(C₃F₇)(PMe₃)(I) (**1c**) with PPh(OMe)₂ in acetone

PPh(OMe)₂ (258.6 mg, 1.520 mmol) was added dropwise to a stirred 40 mL dark green acetone solution of η⁵-CpCo*(C₃F₇)(CO)(I) (334.7 mg, 0.7554 mmol) in a 100 mL Schlenk flask at 50°C until the solution became clear yellow in colour (around 5 h). Removal of volatiles under water aspira-

tor pressure followed by oil pump vacuum overnight left an orange solid, which was purified by PLC on silica gel. Elution with 9/1 acetone/methanol separated (in order of decreasing R_f value) a deep orange zone containing **4c-1** (236.7 mg, 0.4515 mmol), two yellow-green zones containing **6-1** (15.6 mg, 0.0298 mmol) and **6-2** (6.7 mg, 0.0128 mmol), respectively, and an orange zone containing **4c-2** (114.2 mg, 0.2178 mmol).

Crystal structure determination of η^5 - CpCo*(C₃F₇)(PPh(OMe)₂)(P(O)(OMe)Ph), **6-2**

A diastereomeric mixture of **6-1** and **6-2** was prepared as described previously (14). The lower R_f diastereomer was separated using preparative thick-layer radial chromatography and recrystallized by slow evaporation of a methylene chloride – hexane solvent mixture. An orange single crystal was selected and mounted on a glass fibre for X-ray analysis. Crystal data were collected at ambient temperature on a Rigaku AFC6S diffractometer with graphite monochromated Mo K α radiation, $\lambda = 0.71069$ Å, and a 2 kW sealed tube generator using the ω scan technique to a maximum 2θ value of 50.0°. Positional parameters and selected bond distances and angles are given in Tables 5 and 6, respectively. Cell constants and an orientation matrix for data collection were determined from least-squares refinement using the setting angles of the 20 carefully centered reflections in the range $9.22 < 2\theta < 17.73^\circ$ and are given in Table 7. The space group $P\bar{1}$ (no. 2) was assigned on the basis of systematic absences and on the successful solution and refinement of the structure. Omega (ω) scans of several intense reflections, made prior to data collection, had an average width at half-height of 0.31° with a take-off angle of 6.0°. Scans of $(1.47 + 0.30 \tan \theta)^\circ$ were made at a speed of 4.0°/min (in ω). Weak reflections ($I < 10.0\sigma(I)$) were rescanned (max 2) and the counts accumulated to assure good counting statistics. Stationary counts were recorded on each side of the reflection. The ratio of peak counting time to background counting time was 2:1.

The linear absorption coefficient for Mo K α is 8.7 cm⁻¹. An empirical absorption correction, based on azimuthal scans of several reflections, was applied, resulting in transmission factors ranging from 0.95 to 1.00. The data were corrected for Lorentz and polarization effects. A correction for secondary extinction was applied with coefficient = 0.25290 ∓ 10^{-6} . The structure was solved by direct methods (45) using the Molecular Structure Corporation TEXSAN software. Non-hydrogen atoms were refined anisotropically. Idealized hydrogen atoms were included at the calculated positions and were not refined.

Tables of atomic coordinates, bond distances and angles, and torsion angles for η^5 -CpCo*(C₃F₇)(PPh(OMe)₂)(P*(O)-Ph(OMe)), **6-2**, have been deposited as supplementary material.²

² Copies of material on deposit may be purchased from: The Depository of Unpublished Data, Document Delivery, CISTI, National Research Council Canada, Ottawa, Canada K1A 0S2. The tables of atomic coordinates and bond lengths and angles have also been deposited with the Cambridge Crystallographic Data Centre, and can be obtained on request from The Director, Cambridge Crystallographic Data Centre, University Chemical Laboratory, 12 Union Road, Cambridge, CB2 1EZ, U.K. Structure factor tables are no longer being deposited, but may be obtained from the author.

Acknowledgement

We thank the Natural Sciences and Engineering Research Council of Canada (NSERC) for a Grant to C.J. and Memorial University for financial support.

References

1. T.B. Brill and S.J. Landon. *Chem. Rev.* **84**, 577 (1984).
2. H. Brunner, C.R. Jablonski, and P.G. Jones. *Organometallics*, **7**, 1283 (1988).
3. S.J. Landon and T.B. Brill. *J. Am. Chem. Soc.* **104**, 6571 (1982).
4. S.J. Landon and T.B. Brill. *Inorg. Chem.* **23**, 1266 (1984).
5. Z. Zhou, C. Jablonski, and J. Bridson. *Organometallics*, **13**, 781 (1994).
6. Z. Zhou, C. Jablonski, and J. Bridson. *Organometallics*, **12**, 3677 (1993).
7. H. Nakazawa, M. Yamaguchi, K. Kubo, and K. Miyoshi. *J. Organomet. Chem.* **428**, 145 (1992).
8. H. Nakazawa, Y. Kadoi, and K. Miyoshi. *Organometallics*, **8**, 2851 (1989).
9. H. Nakazawa, Y. Kadoi, T. Mizuta, K. Miyoshi, and H. Yoneda. *J. Organomet. Chem.* **366**, 333 (1989).
10. E.V. Schleman and T.B. Brill. *J. Organomet. Chem.* **323**, 103 (1987).
11. H. Nakazawa, T. Fujita, K. Kubo, and K. Miyoshi. *J. Organomet. Chem.* **473**, 243 (1994).
12. C. Leiva, K. Mossert, A.H. Klahn, and D. Sutton. *J. Organomet. Chem.* **469**, 69 (1994).
13. B.J. Boone, C.R. Jablonski, P.G. Jones, M.J. Newlands, and Y.F. Yu. *Organometallics*, **12**, 3042 (1993).
14. C.R. Jablonski, H.Z. Ma, Z. Chen, R.C. Hynes, J.N. Bridson, and M.P. Bubenik. *Organometallics*, **12**, 917 (1993).
15. D.G. Gilheaney. *In The chemistry of organophosphorus compounds*. Vol. 2. John Wiley, New York. 1992. pp. 1–52.
16. D.M. Roundhill, R.P. Sperline, and W.B. Beaulieu. *Coord. Chem. Rev.* **26**, 263 (1978).
17. B. Walther. *Coord. Chem. Rev.* **60**, 67 (1984).
18. S. Neumann, D. Schomburg, and R. Schmutzler. *J. Chem. Soc. Chem. Commun.* 848 (1979).
19. T.E. Sloan. *Top. Stereochem.* **12**, 1 (1981).
20. C. Lecomte, Y. Dusavsoy, J. Protas, J. Tirouflet, and A. Dormand. *J. Organomet. Chem.* **73**, 67 (1974).
21. P. Mata, A.M. Lobo, C. Marshall, and A.P. Johnson. *Tetrahedron: Asymmetry*, **4**, 657 (1993).
22. H. Nakazawa, K. Morimasa, Y. Kushi, and H. Yoneda. *Organometallics*, **7**, 458 (1988).
23. J. Reinhard, M. Luksza, W. Malisch, D. Kempf, and G. Kuenzel. *J. Organomet. Chem.* **266**, C22 (1984).
24. H.A. Kaul, D. Greissing, M. Luksza, and W. Malisch. *J. Organomet. Chem.* **228**, C29 (1982).
25. W. Malisch and A. Meyer. *J. Organomet. Chem.* **198**, C29 (1980).
26. H. Brunner. *Adv. Organomet. Chem.* **18**, 151
27. J.M. O'Connor and C.P. Casey. *Chem. Rev.* **87**, 307 (1987).
28. H. Brunner and M. Lappus. *Angew. Chem. Int. Ed. Engl.* **11**, 923 (1972).
29. H. Brunner and H. Vogt. *Chem. Ber.* **114**, 2186 (1981).
30. G.W. Parshall and S.D. Ittel. *In Homogeneous catalysis — The application and chemistry of catalysis by soluble transition metal complexes*. 2nd ed. John Wiley & Sons, New York. 1992.
31. M.A. Dewey, Y.L. Zhou, Y.M. Liu, and J.A. Gladysz. *Organometallics*, **12**, 3924 (1993).
32. M. Saunders, K.N. Houk, Y.-D. Wu, W.C. Still, M. Lipton, G. Chang, and W.C. Guida. *J. Am. Chem. Soc.* **112**, 1419 (1990).

33. J.J. Gajewski, K.E. Gilbert, and J. McKelvey. *In* Advances in Molecular Modeling. Vol. 2. JAI Press Inc., Greenwich, Conn. 1990. pp. 65-92.
34. S.C. Mackie and M.C. Baird. *Conn. Organometallics*, **11**, 3712 (1992).
35. J. Polowin, S.C. Mackie, and M.C. Baird. *Conn. Organometallics*, **11**, 3724 (1992).
36. B.K. Blackburn, S.G. Davies, K.H. Sutton, and M. Whittaker. *Chem. Soc. Rev.* **17**, 147 (1988).
37. B.K. Blackburn, S.G. Davies, and M. Whittaker. *In* Stereochemistry of organometallic and inorganic compounds. Vol. 3. Elsevier, Amsterdam. 1989. pp. 141-223.
38. H. Brunner, B. Hammer, C. Krueger, K. Angermund, and I. Bernal. *Organometallics*, **4**, 1063 (1985).
39. S.E. Garner and A.G. Orpen. *J. Chem. Soc. Dalton Trans.* 533 (1993).
40. H. Brunner, R. Oeschey, and B. Nuber. *Angew. Chem. Int. Ed. Engl.* **33**, 866 (1994).
41. J.I. Seeman. *Chem. Rev.* **83**, 83 (1983).
42. C.R. Jablonski, T. Burrow, and P.G. Jones. *J. Organomet. Chem.* **370**, 173 (1989).
43. C.R. Jablonski, H.Z. Ma, and R.C. Hynes. *Organometallics*, **11**, 2796 (1992).
44. R.B. King, P.M. Treichel, and F.G.A. Stone. *J. Am. Chem. Soc.* **83**, 3593 (1961).
45. C.J. Gilmore. *J. Appl. Crystallogr.* **17**, 42 (1984).